




ARTICLE

DOI: 10.1038/s41467-017-00874-0

OPEN

All-optical regenerator of multi-channel signals

Lu Li^{1,3}, Pallavi G. Patki^{1,4}, Young B. Kwon^{1,5}, Veronika Stelmakh ^{1,6}, Brandon D. Campbell¹,
Muthiah Annamalai ^{1,7}, Taras I. Lakoba² & Michael Vasilyev ¹

One of the main reasons why nonlinear-optical signal processing (regeneration, logic, etc.) has not yet become a practical alternative to electronic processing is that the all-optical elements with nonlinear input-output relationship have remained inherently single-channel devices (just like their electronic counterparts) and, hence, cannot fully utilise the parallel processing potential of optical fibres and amplifiers. The nonlinear input-output transfer function requires strong optical nonlinearity, e.g. self-phase modulation, which, for fundamental reasons, is always accompanied by cross-phase modulation and four-wave mixing. In processing multiple wavelength-division-multiplexing channels, large cross-phase modulation and four-wave mixing crosstalks among the channels destroy signal quality. Here we describe a solution to this problem: an optical signal processor employing a group-delay-managed nonlinear medium where strong self-phase modulation is achieved without such nonlinear crosstalk. We demonstrate, for the first time to our knowledge, simultaneous all-optical regeneration of up to 16 wavelength-division-multiplexing channels by one device. This multi-channel concept can be extended to other nonlinear-optical processing schemes.

¹Department of Electrical Engineering, University of Texas at Arlington, Arlington, TX 76019, USA. ²Department of Mathematics and Statistics, University of Vermont, Burlington, VT 05401, USA. ³Present address: TE SubCom, Eatontown, NJ 07724, USA. ⁴Present address: Infinera Corp., Bangalore 560025, India. ⁵Present address: Lightwave Logic, Inc., Longmont, CO 80501, USA. ⁶Present address: Department of Electrical Engineering and Computer Science, Massachusetts Institute of Technology, Cambridge, MA 02139, USA. ⁷Present address: Synopsys, Inc., Mountain View, CA 94043, USA. Lu Li and Pallavi G. Patki contributed equally to this work. Correspondence and requests for materials should be addressed to M.V. (email: vasilyev@uta.edu)

All-optical regeneration is a striking example of the need for wavelength-division-multiplexing (WDM) compatibility in nonlinear-optical signal processing. All-optical regenerators reset to their original shape the signals that have accumulated noise and distortion due to propagation in fibre communication lines. In the simplest case of 2R regenerators, re-amplification and re-shaping takes place. In 3R regenerators, a function of re-timing is added. Although all-optical regenerators can be data-rate independent and work with much higher (Terabits per second) maximum rates than their optoelectronic counterparts, the latter offer more advanced capabilities (e.g. forward error correction) and lower manufacturing cost. Thus, to be practically viable, one all-optical regenerator must be able to replace a large number of optoelectronic regenerators, which makes its compatibility with WDM the most important challenge^{1, 2}. This challenge, however, is of fundamental nature, because the threshold-like input-output power transfer function of a 2R regenerator requires strong optical nonlinearity, which necessarily leads to cross-phase modulation (XPM) and four-wave mixing (FWM) interaction among the WDM channels. While the re-timing function of 3R regenerator can, at least in principle, be performed for all WDM channels by a single device^{3–6} (though under rather impractical assumptions of synchronised clock rates for all channels), the WDM operation of a 2R regenerator has remained a fundamental obstacle up until now.

The efforts on overcoming this problem have intensified over the last decade and can be roughly arranged into three approaches. The first approach is to use spatial degrees of freedom to isolate the WDM channels from interacting with one another, which means that the channels are de-multiplexed and subsequently processed by separate nonlinear media^{4, 7–10}. Second approach is to employ a single nonlinear medium, but use other degrees of freedom, such as polarisation¹¹ and opposite directions of propagation^{12, 13}, to isolate WDM channels. This approach has led to the demonstration of simultaneous regeneration of four channels in the same nonlinear fibre¹⁴. The third approach is to employ very low spectral efficiency in WDM transmission, which can help minimise interaction among the WDM channels either by placing the channels far from each other in frequency domain, or by separating the bits far from each other in time domain (i.e. using low-duty-cycle pulses). For the time-domain-separation method, the low duty cycle suppresses the interaction by ensuring that neighbouring-channel pulses very rarely overlap in time^{15, 16}. However, the low-duty-cycle pulses require bandwidth greatly exceeding their repetition frequency (and hence greatly exceeding their data rate), i.e. they are not spectrally efficient. Another variant of time-domain-separation method involves interleaving the pulses from different WDM channels in time^{16–19}, but it requires bit synchronisation among the channels, which is not possible to achieve in real communication systems. For frequency-domain-spacing method, the interaction is suppressed by the presence of substantial chromatic dispersion of the fibre, which makes the neighbouring-channel pulse streams rapidly walk off from each other, thereby eliminating FWM and reducing XPM to merely a constant phase shift proportional to the average power of the neighbouring channel. However, the dispersion also causes the different frequency components of the data-carrying pulses within each WDM channel to walk off from each other. This distorts the pulse shape and eliminates the regenerative effect of the optical nonlinearity unless the ratio of the bandwidth of each WDM channel to the inter-channel spacing, known as spectral efficiency, is very small. Thus, none of the approaches discussed above have shown any potential for increasing the number of regenerated channels beyond four, unless the channels carry identical data and/or their bits are synchronised in time^{16, 19, 20}, which is impractical.

A radically different method of WDM regeneration was proposed by us in ref. ²¹. This approach uses the benefits of the dispersive walk-off between the WDM channels to avoid FWM and XPM, but at the same time eliminates the walk-off among the frequency components within each channel to preserve pulse integrity and enable accumulation of large amounts of self-phase modulation (SPM). In order to achieve this, we proposed to make an artificial group-delay-managed (GDM) nonlinear medium consisting of a series of short nonlinear fibre sections separated by spectrally periodic phase filters known as periodic group-delay devices (PGDDs). The GDM medium has chromatic dispersion that is periodic both in propagation direction and in frequency, and is described in detail in the ‘Results’ section. While its unique properties can enable the WDM operation in any SPM-based 2R regenerator, for the purpose of demonstration we focus on the regenerator of on-off-keying (OOK) signals, based on SPM spectral broadening followed by spectral filtering (Mamyshev regenerator scheme²²).

In this paper, we report the demonstration of the first, to our knowledge, truly multi-channel 2R regenerator, which uses the Mamyshev scheme enabled by the GDM nonlinear medium. The presented work consists of two parts: in the first one the regeneration with GDM medium is studied by placing one GDM unit cell consisting of a fibre section and a PGDD into a recirculating loop^{23, 24} and letting the signals propagate through this cell multiple times; in the second one we use the obtained insights to build the first stand-alone GDM-enabled Mamyshev regenerator and demonstrate simultaneous regeneration of 16 WDM channels in it. We have reported preliminary 3- and 12-channel stand-alone regeneration data in two recent conference papers^{25, 26}. This paper presents the experiment with optimised dispersion map and Raman amplification, yielding the eye-opening improvements that are significantly greater and more equalised among the channels, and resulting in regeneration of the largest number (16) of WDM channels to date. (While this manuscript was under review, we learned of a more recent work reporting regeneration of 16 channels with 50-GHz spacing, albeit requiring bit synchronisation among all channels: Guan et al.²⁷.) The GDM-based approach can be straightforwardly extended to higher channel counts and higher symbol rates, and we believe it can also be adapted for regeneration of more advanced modulation formats.

Results

Group-delay-managed nonlinear medium. Our approach, originally proposed in ref. ²¹, uses the dispersive walk-off between the WDM channels to avoid FWM and XPM, but at the same time produces no walk-off among the frequency components within each channel, which preserves pulse integrity and enables accumulation of large amounts of SPM. In order to achieve this, we split the nonlinear fibre used for 2R regeneration into a series of short sections separated by spectrally periodic phase filters known as PGDDs, as shown in Fig. 1a. Such filters, usually made of several cascaded Gires–Tournois etalons^{28, 29}, have sawtooth-like group-delay spectra (Fig. 1b). When the PGDD spectrum is added to a straight-line (i.e. constant-dispersion) group-delay spectrum of a section of the nonlinear fibre, the resulting group-delay spectrum of the ‘fibre+PGDD’ combination exhibits staircase-like behaviour (Fig. 1b). This ensures equal delays (i.e. no dispersion) among all frequency components within each channel, thereby maximising SPM, but at the same time introduces temporal walk-off between different WDM channels, which reduces XPM and FWM. When multiple ‘fibre+PGDD’ unit cells are concatenated, such walk-off is accumulated, effectively resulting in the creation of a new artificial nonlinear medium with

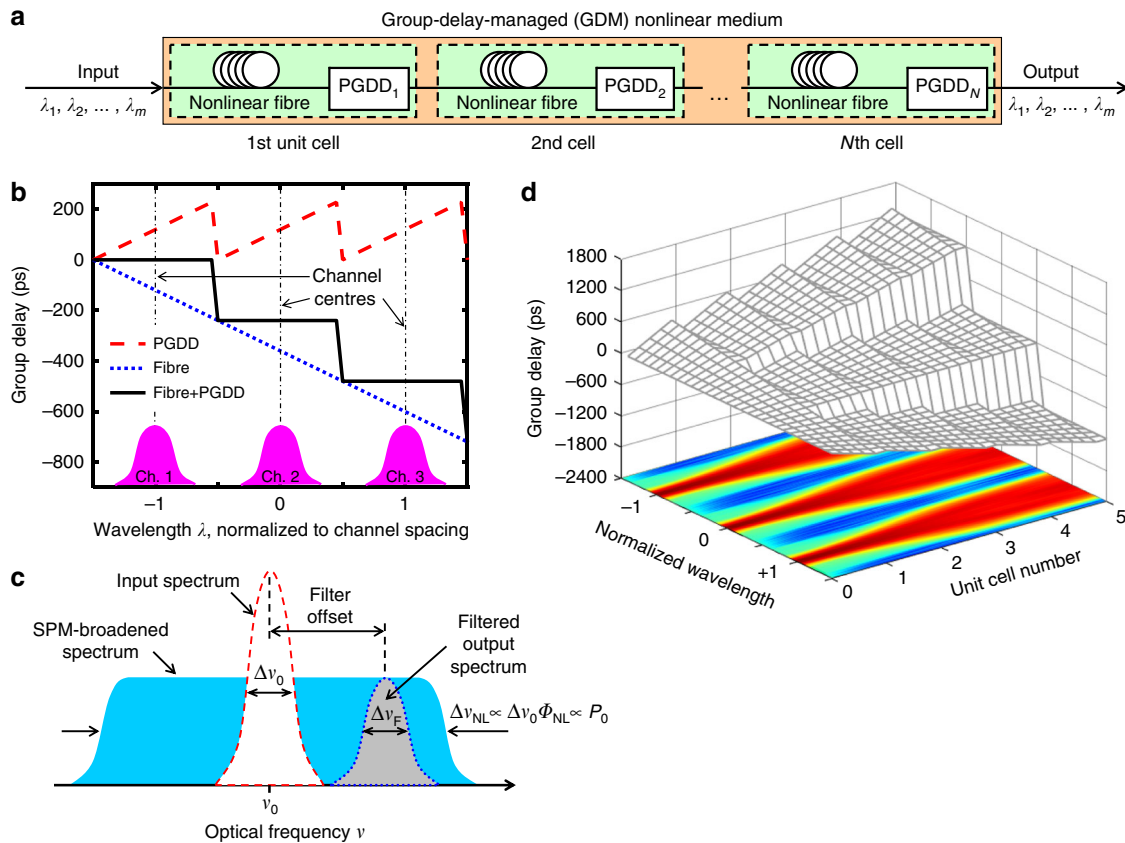


Fig. 1 Principle of multi-channel 2R regeneration. **a** Group-delay-managed (GDM) medium is made by concatenation of N ‘fibre + periodic group-delay device (PGDD)’ unit cells and processes m WDM channels. **b** Each cell has a staircase-like group-delay spectrum (whose derivative is dispersion), ensuring strong nonlinearity within each channel, but suppressed nonlinear interactions among the channels. Group-delay spectra are shown for three adjacent WDM channels. **c** Single-channel Mamyshev 2R regenerator is based on signal’s spectral broadening by self-phase modulation (SPM), followed by off-centre bandpass filtering. **d** Propagation in the GDM medium results in group-delay walk-off between the adjacent channels (wavelength is normalised to channel spacing) and allows their simultaneous broadening by the SPM without nonlinear inter-channel crosstalk. The coloured map underneath represents evolution of power spectral densities of the three channels. Group delay values in **b**, **d** assume the channel spacing of 200 GHz (1.6 nm) and fibre with dispersion $D = -120$ ps nm⁻¹ km⁻¹ and section length of 1.25 km

large group-velocity dispersion among different WDM channels and with no dispersion within each channel. In such a medium, which we refer to as ‘GDM nonlinear medium,’ the benefits of large SPM can be enjoyed simultaneously by each of many WDM channels without suffering from the FWM and XPM. In this paper we focus on a GDM medium based on nonlinear fibres and commercially available PGDDs^{29, 30}. In the future, it might be possible to implement the entire GDM on a chip using integrated-photonics solutions for both nonlinear^{31, 32} and PGDD^{33–35} functions.

The use of bit walk-off to suppress XPM was originally proposed for conventional long-haul communication lines^{36, 37} and later was demonstrated with PGDDs for dispersion-managed soliton transmission^{38, 39}. The long-haul communication lines, however, operate in the regime where the nonlinearities are weak, whereas 2R regeneration inherently relies on large SPM, i.e. operates in a strongly nonlinear regime. We found the optimum parameters of operation for the latter regime⁴⁰, which indicate that an excellent 2R performance, which is also very robust with respect to perturbations of the experimental parameters, can be obtained with as few as five or six ‘fibre + PGDD’ unit cells with anomalous net dispersion of the cell and large normal dispersion of the nonlinear fibre.

The GDM nonlinear medium can enable the WDM operation in any SPM-based 2R regenerator or other optical signal processor. In this paper we report its application to a particular

scheme known as the Mamyshev regenerator²². The operation of the latter is illustrated in Fig. 1c for the case of a single channel. After propagation in nonlinear fibre, a noisy input pulse (‘ONE’ symbol) with original bandwidth $\Delta\nu_0$ experiences SPM-caused spectral broadening so that the width of the broadened spectrum $\Delta\nu_{NL}$ is proportional to the input pulse’s peak power P_0 while the power spectral density of the broadened spectrum is virtually independent of the input power. Hence, by selecting a portion of the broadened spectrum by an optical bandpass filter (OBPF), one can obtain an output pulse of approximately the same duration as the input pulse (if OBPF width $\Delta\nu_F \approx \Delta\nu_0$), but with the magnitude that does not change with input power fluctuations (regeneration of ‘ONES’ symbols). On the other hand, any noise between the pulses (i.e. taking place of ‘ZERO’ symbols) is too weak to cause SPM broadening and is confined within the input signal’s bandwidth. If the OBPF centre frequency is offset from the centre of the input signal’s spectrum, the noise between the pulses is not transmitted to filter’s output, which constitutes the regeneration of ‘ZERO’ symbols. For proper operation, the Mamyshev scheme requires large amount of SPM (3...12 radians of nonlinear phase shift Φ_{NL}). Figure 1d illustrates application of the GDM medium to the Mamyshev regenerator.

The compatibility of the Mamyshev regenerator with conventional dispersion management has been experimentally demonstrated for a single channel⁴¹ and later investigated with three to four channels^{15, 42}. These experiments used alternating

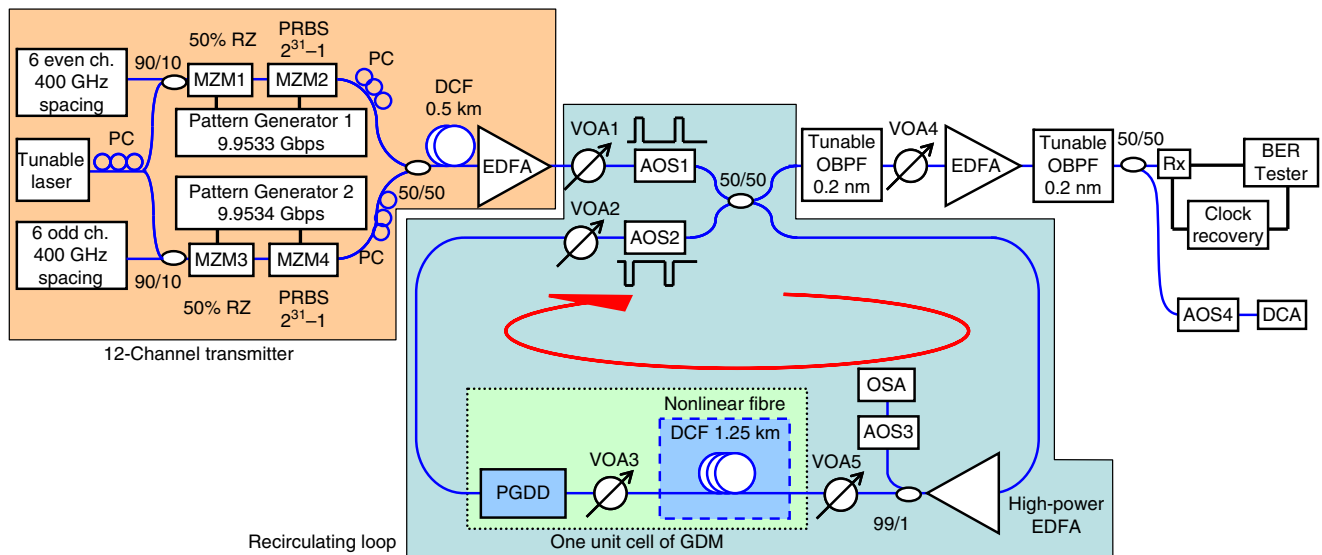


Fig. 2 Experimental recirculating-loop setup. 10-Gbps-modulated signals from 12-channel transmitter enter the recirculating loop containing one GDM unit cell. After five circulations the signals are filtered and detected by a pre-amplified receiver (Rx). The tunable laser is used to generate $\pm 25\%$ amplitude jitter when it is tuned to the wavelength of the signal channel to be measured. MZM: electro-optic Mach-Zehnder modulator, EDFA: erbium-doped fibre amplifier, PC: polarisation controller, AOS: acousto-optic switch, VOA: variable optical attenuator, DCF: dispersion-compensating fibre, OSA: optical spectrum analyser, OBPF: optical bandpass filter, DCA: digital communication analyser

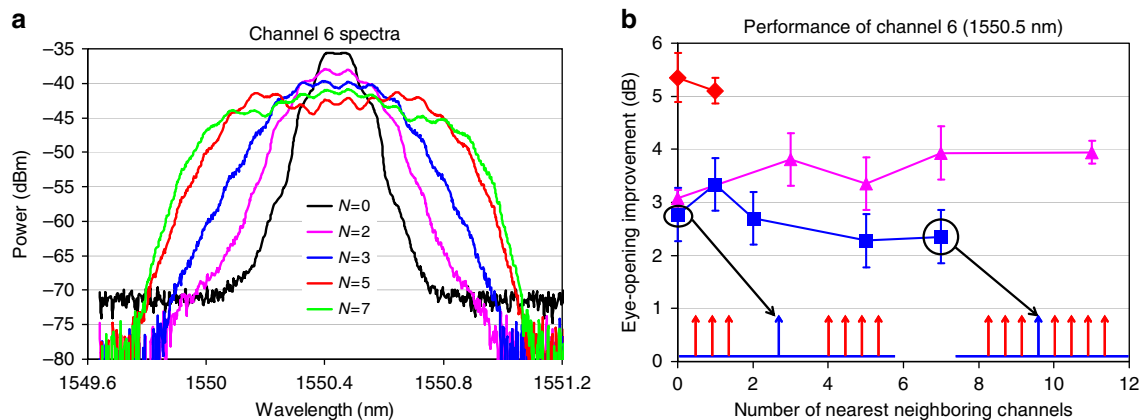


Fig. 3 Multi-channel 2R regeneration in the recirculating loop. **a** SPM-broadened spectra of the central (1550.5 nm) channel (out of 12 channels total) after N circulations, obtained with the resolution bandwidth of 0.1 nm. **b** Eye-opening improvement at $\text{BER} = 10^{-9}$ for the central 1550.5-nm channel after $N = 5$ circulations versus the number of other simultaneously regenerated channels. Different-coloured traces in **b** describe three separate experiments using different EDFAs in the loop and should not be compared to one another. Red diamonds correspond to the increase from 1 to 2 and the purple triangles—to the increase from 1 to 12 in the total number of consecutive 200-GHz-spaced WDM channels. Blue squares correspond to the change in the number of the central channel's closest neighbours on the 200-GHz-spaced grid from 0 to 7, while the total number of channels is kept at 8. Error bars are obtained from the linear fits to BER curves (red diamonds, first and last purple triangles) and from power measurement uncertainties (blue squares, three middle purple triangles)

normal- and anomalous-dispersion fibres and did not involve PGDDs. Such conventional dispersion management schemes do not monotonically accumulate walk-off between channels and, hence, are unable to sufficiently suppress XPM and FWM. As a result, these experiments could not be extended to multi-channel operation.

In this paper, we demonstrate multi-channel 2R regeneration in the Mamyshev scheme enabled by the GDM nonlinear medium. In all presented experiments the nonlinear fibre is the conventional dispersion-compensating fibre (DCF) with nonlinear constant $\gamma \approx 5 \text{ (W km)}^{-1}$, dispersion $D = -120 \text{ ps nm}^{-1} \text{ km}^{-1}$, and attenuation $\approx 0.5 \text{ dB km}^{-1}$. All signals are OOK modulated by a $2^{31}-1$ pseudo-random bit sequence (PRBS) and carved into 50% return-to-zero (RZ) pulses. To ensure the worst case of

inter-channel nonlinearities (XPM and FWM), all WDM signals are co-polarised. In order to properly characterise the 2R regeneration performance, we decorrelate the clock frequencies and the bit patterns between the neighbouring channels (see 'Methods' for more details). Without proper clock decorrelation, one is likely to observe unrealistically optimistic regeneration performance (e.g. when the 50% RZ pulses from the neighbouring channels are interleaved in time), which cannot be achieved in a practical communications system, where the channels have independent (uncorrelated) clocks.

Multi-channel regeneration in a loop-based GDM medium. In order to be able to easily vary the number of 'fibre + PGDD' unit

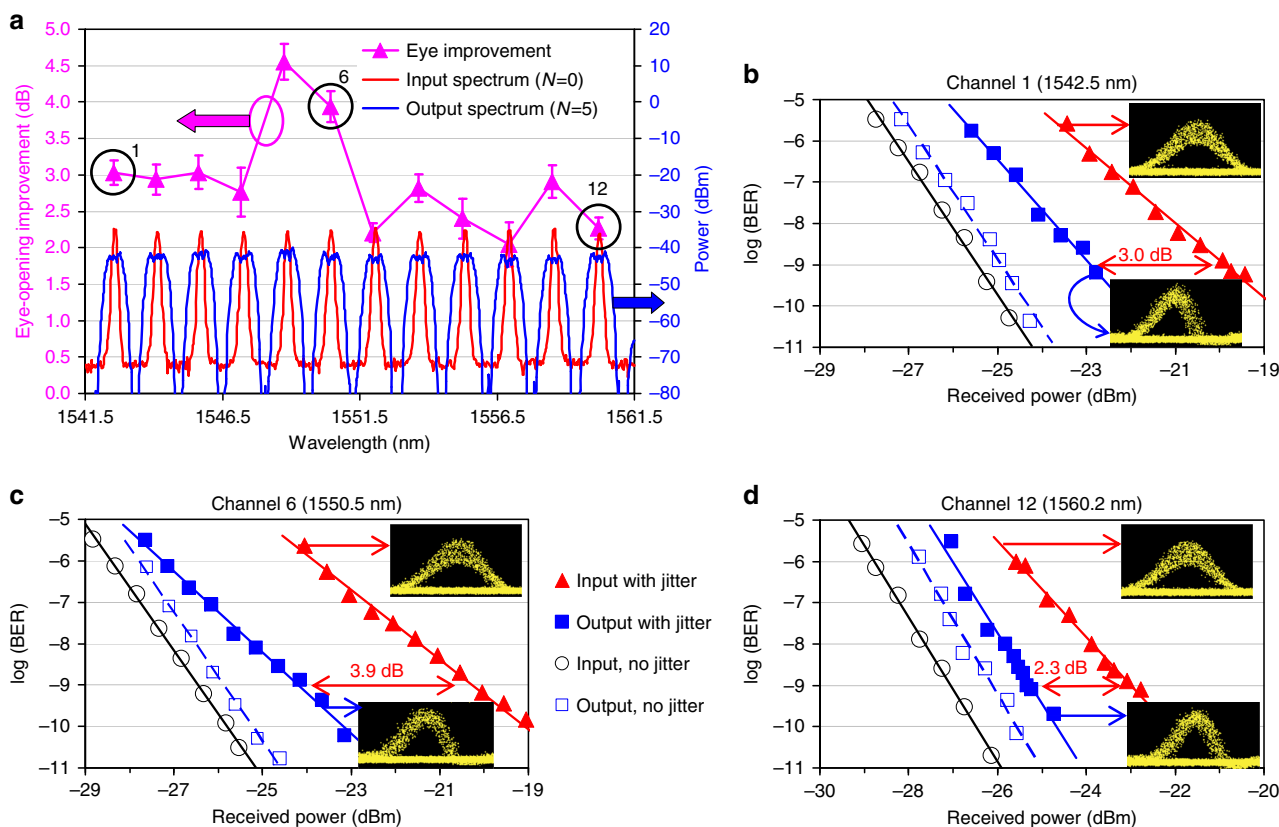


Fig. 4 Results of 12-channel 2R regeneration in the recirculating loop. **a** Eye-opening improvements at $\text{BER} = 10^{-9}$ for 12 simultaneously regenerated channels (left axis); 12-channel spectra at the input (blue) and output (red) of the regenerator (right axis), obtained with the resolution bandwidth of 0.1 nm. N is the number of circulations. Error bars are obtained from the linear fits to BER curves. Numbered circles indicate the channels shown in **b-d**. **b-d** BER curves and eye diagrams for amplitude-jitter-degraded signals before (red triangles) and after the regeneration (blue squares) for 1542.5-nm (**b**), 1550.5-nm (**c**) and 1560.2-nm (**d**) channels. BERs for signals without amplitude jitter are also shown (black open circles—before and blue open squares—after the regeneration). **b-d** Share common legend. The eye diagrams (insets in **b-d**) exhibit significant reduction in the amplitude jitter after the regeneration

cells in the regenerator without drastic increase in the required resources, and to experimentally confirm the parameters of the theoretically predicted regime⁴⁰ of multi-channel regeneration in the GDM medium, we have built a recirculating loop^{23, 24}, where we used only one ‘fibre + PGDD’ unit cell and passed the signals through it multiple times (Fig. 2) to achieve the effect of concatenating multiple identical cells. After each pass (circulation), the spectrum of each WDM channel is increasingly broadened by SPM, until it completely fills the passband width of the PGDD’s amplitude response after five circulations (the PGDD in this experiment has a periodic bandpass amplitude characteristic with -1-dB width of 100 GHz), as shown in Fig. 3a. Hence, using a 10 Gigabit-per-second (Gbps) signal after five circulations as the regenerated output, we have studied the regeneration performance with various numbers of channels (Fig. 3b). Although 2R regeneration cannot improve the intrinsic bit-error rate (BER) of the signal, the compression of noise of ‘ZERO’ and ‘ONE’ symbols makes the signal more robust with respect to subsequent noise addition. This improvement (a.k.a. ‘eye-opening improvement,’ because it increases the opening between the ‘ZERO’ and ‘ONE’ levels on the eye diagram) is quantified by the reduction of the signal power level at the receiver’s optical pre-amplifier entrance that is required to obtain $\text{BER} = 10^{-9}$. While the merits of a regenerator are ultimately determined by the reach extension it offers to a specific real transmission system in the field, the eye-opening improvement is the widely accepted laboratory measure of the regenerator’s ability to suppress the signal’s impairments

and hence improve the system performance. In three separate experiments, we have found that the eye-opening improvement of the central channel degraded by amplitude jitter does not show any noticeable degradation when the number of WDM channels on a 200-GHz-spaced grid is increased from 1 to 2 (red diamonds in Fig. 3b), from 1 to 12 (purple triangles), or when the number of the channel’s closest neighbours on this grid is changed from 0 to 7 while keeping the total number of channels at 8 (blue squares). In general, the negative impact of XPM and FWM from neighbouring channels on the performance of a given regenerated channel quickly diminishes with the increased frequency separation between the channels. Thus, only a few (5–7) closest neighbours have a potential to degrade the signal channel’s regeneration performance. Our GDM method strongly suppresses this degradation: as the results in Fig. 3b show, the performance is not degraded as we change the number of closest neighbour channels from 0 to 11. Thus, in line with our theoretical prediction in ref. 21, these results experimentally demonstrate that there is no fundamental XPM or FWM limit on the number of channels regenerated in our scheme, i.e. adding more channels would not increase XPM or FWM impairments.

The most important results of the recirculating-loop experiment are presented in Fig. 4a–d, demonstrating 2R regeneration of 12 10-Gbps channels with 200-GHz spacing. The data in Fig. 4a, obtained from comparing the curves of BER versus receiver pre-amplifier’s input power (examples of which are given in Fig. 4b–d), clearly indicate that the regenerator improves eye

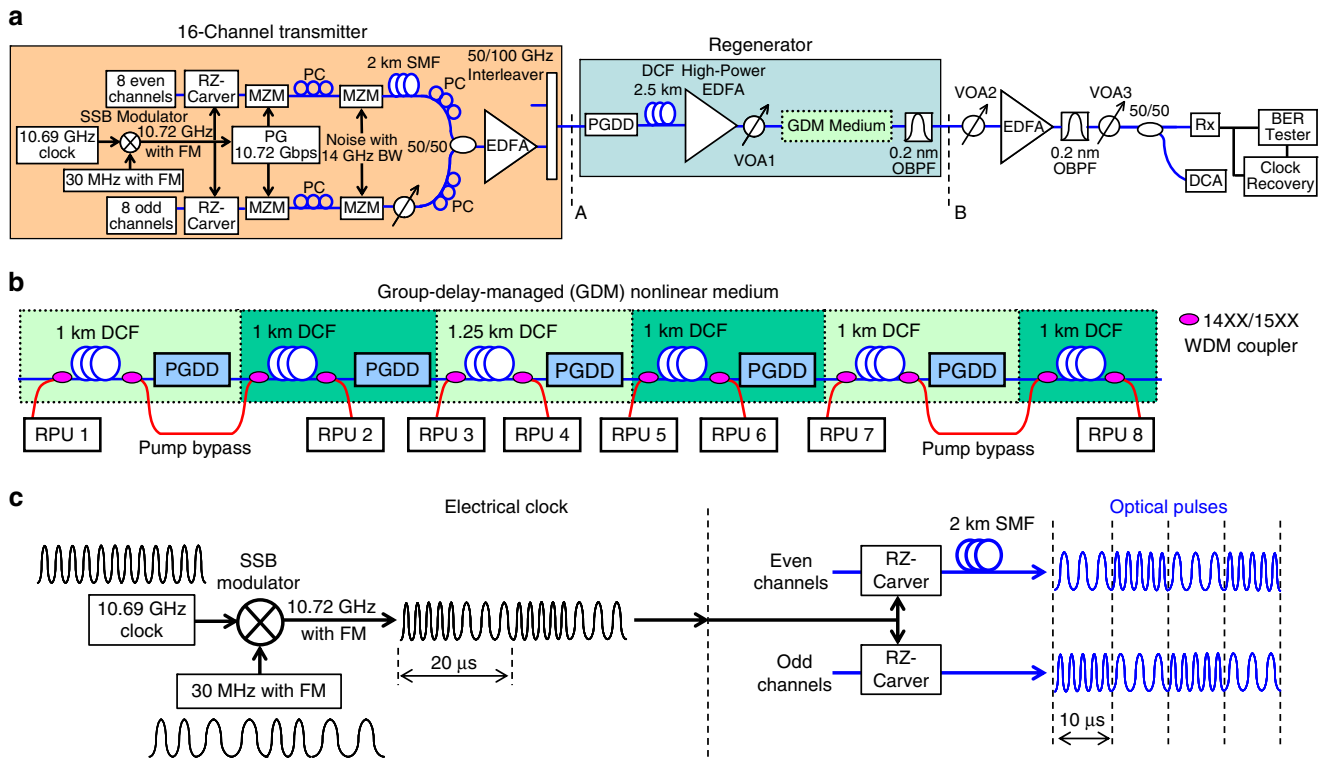


Fig. 5 Stand-alone regenerator setup. **a** 10-Gbps-modulated signals from a 16-channel transmitter enter the regenerator, and their performance is characterised by a pre-amplified receiver. **b** GDM medium in the stand-alone regenerator consists of six Raman-pumped sections of DCF, separated by five PGDDs. PG: pattern generator, SSB: single sideband, SMF: single-mode fibre, RPU: Raman pump unit. **c** Decorrelation of the even- and odd-channel clock frequencies by frequency modulation (FM) of a single clock source

opening by more than 2 dB for all 12 channels. The eye diagrams in the insets of Fig. 4b–d also show significant reduction of the amplitude jitter after the regeneration. The number of channels in this experiment has been limited by the gain-flattened bandwidth of our high-power erbium-doped fibre amplifier (EDFA) (1542–1560 nm) and the 200-GHz channel spacing of the PGDD. The role of gain flattening is evident in Fig. 4a by the better performance of channels 5 and 6, for which the EDFA gain ripple is minimal. This results in the smallest input-to-output power excursion, a more even distribution of the SPM generation among all circulations, and nearly ideal regeneration conditions for these two channels.

Demonstration of a stand-alone multi-channel 2R regenerator.

With the insights gained from the recirculating-loop experiments, we have built a stand-alone 2R regenerator (Fig. 5a) consisting of five PGDDs and six sections of nonlinear fibre (Fig. 5b), described in greater detail in ‘Methods’. Although an ideal PGDD is a pure all-pass filter and there are no fundamental limits on making it virtually lossless, the PGDDs that are commercially available today have finite insertion losses of 3–5 dB, primarily owing to the lack of market incentive to further reduce the loss in their current application (dispersion compensation at the loss-tolerant mid-stage of an EDFA). To compensate for the loss of the PGDDs, nonlinear fibre, couplers, and splices, and to achieve similar amounts of SPM in all fibre sections, we use bi-directional distributed Raman amplification in all sections of the nonlinear fibre. The number of regenerated WDM channels in our experiment is limited by the available Raman pump wavelengths and powers, which determine the spectral shape and magnitude of the saturated Raman gain. In order to avoid confusing 2R

regeneration with artifacts of Raman gain saturation (which can suppress low-frequency amplitude jitter), we introduce fast amplitude fluctuations by modulating all channels with broadband (14-GHz-wide) Nyquist–Johnson electronic noise. The multi-channel regeneration is characterised by comparing the eye diagrams and ‘BER versus receiver input power’ curves between the regenerator input (point A in Fig. 5a) and regenerator output (point B in Fig. 5a) for all channels.

The experimental results shown in Figs. 6 and 7 indicate similar amounts of the SPM-induced spectral broadening and similar eye-opening improvements for all 16 regenerated channels. In addition to presenting 16-channel spectra in Fig. 6a, we show detailed view of the spectra of four representative channels (channels 2, 6, 12 and 16) in Fig. 6b–e to illustrate that they indeed have similar shapes and similar amounts of nonlinear spectral broadening. The eye diagrams of these channels (insets in Fig. 6b–e) also exhibit similar and clearly noticeable amounts of the amplitude noise suppression by the regenerator. Figures 7a, b indicate that the eye-opening improvements for all 16 channels are 4.8 dB or better. Building upon the 12-channel recirculating-loop results, this 16-channel experiment represents the first, to the best of our knowledge, demonstration of a truly multi-channel 2R regenerating device. Moreover, it uses 100-GHz WDM channel spacing, which, as of the manuscript’s submission time, is the narrowest channel spacing among any 2R regenerators processing more than one WDM channel.

We emphasise that the number of channels in this experiment is not constrained by any conceptual limitations of the GDM approach, and is only limited by the bandwidth of the practical Raman amplifiers available in our lab. Hence, we expect this approach to be scalable to much higher channel counts when wider-bandwidth amplifiers are used.

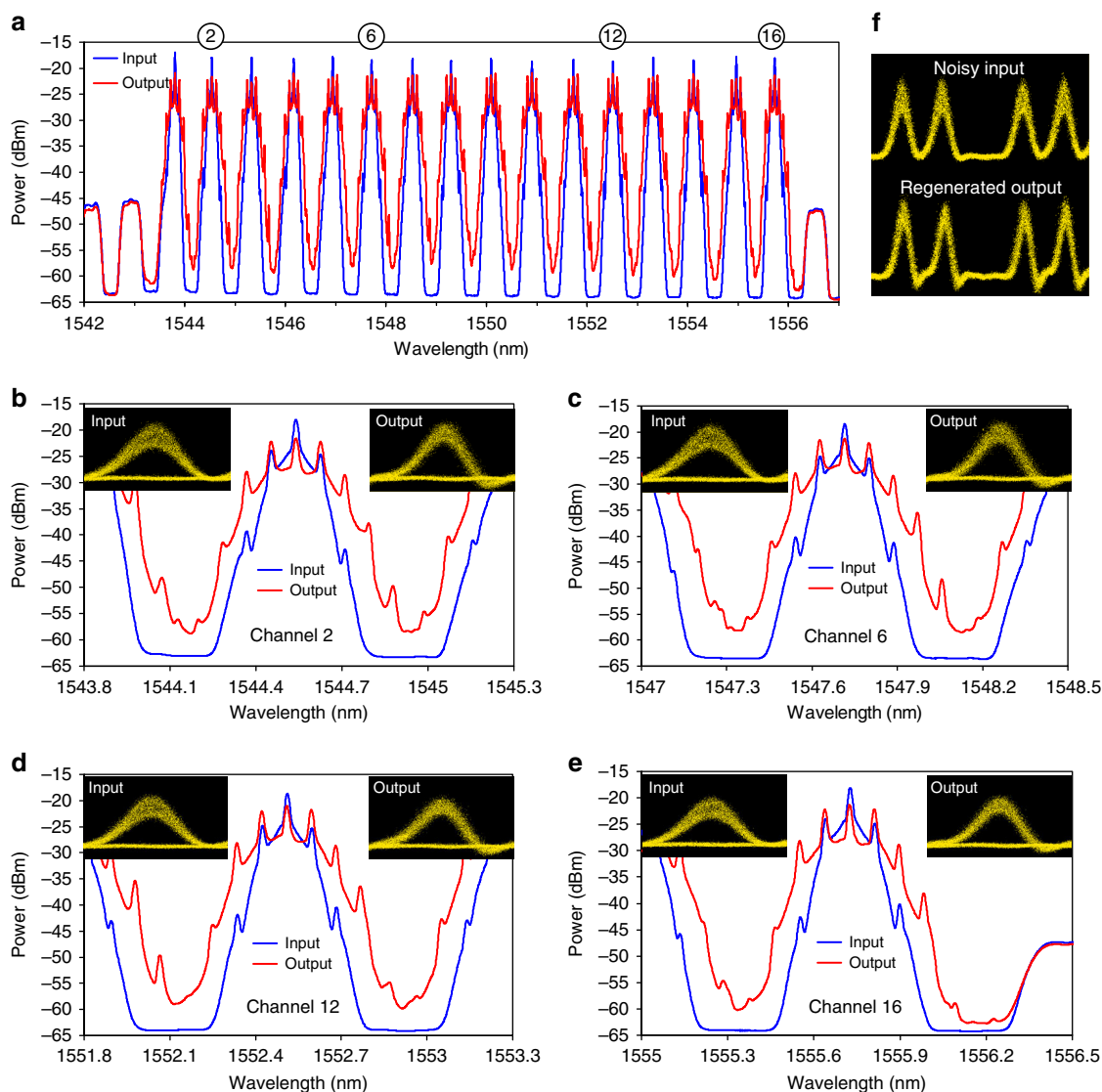


Fig. 6 Spectra and eye-diagrams before and after the stand-alone 2R regenerator. **a–e** Optical spectra of the noise-degraded signals at the regenerator input (blue) and output (red) for all 16 channels (**a**) and four representative channels (detail view, **b–e**), obtained with the resolution bandwidth of 0.016 nm. Corresponding eye diagrams are shown as insets. Encircled numbers at the top of **a** show positions of the four channels. **f** 5-bit pattern before and after regeneration (1555.75-nm channel)

Discussion

There are two main reasons why the measured eye-opening improvements differ between the recirculating-loop and stand-alone regenerator experiments: (a) extra loss per unit cell (i.e. per circulation) inherent to operation of the recirculating loop and (b) different types of signal degradation used in the two experiments (see ‘Methods’ for more details), with broadband noise used in the stand-alone regenerator experiment having stronger impact on the BER. We would also like to note that the broadband noise is not only the most challenging, but also the most important impairment to regenerate. Indeed, the linear-optical transmission-line impairments (e.g. chromatic dispersion) can be easily overcome by simple multi-channel-compatible means, and many nonlinear-optical impairments (e.g. nonlinear inter-channel crosstalk) can be compensated in the near future either by digital back-propagation techniques⁴³ or by multi-channel-compatible mid-span spectral inversion^{44–46}. On the other hand, the distributed nonlinear interaction of the signal with the broadband noise has been shown to be the most fundamental

capacity-limiting transmission-line impairment that can only be undone by regeneration^{47, 48}. It is also worth noting that, although our artificial degradations in both recirculating-loop and stand-alone regeneration experiments primarily affect the amplitude of the ‘ONES’ symbols, the ‘ZEROS’ symbols still carry the usual impairments inherent to transmission systems, such as finite (~ 13 dB) extinction ratio of the modulators, accumulation of the amplified spontaneous emission noise, etc. Thus, even though the ‘ZEROS’ symbols are not artificially degraded, and their noise in the eye-diagram pictures is partially obscured by the receiver noise of the digital communication analyser (DCA), the measured BERs and eye-opening improvements represent the net performance contributed by both ‘ONES’ and ‘ZEROS’. The ability of a GDM-based Mamyshev regenerator to improve the signal having strongly artificially degraded ‘ZEROS’ was previously demonstrated for a single channel⁴¹.

By employing lower-loss PGDDs and wider-bandwidth optical amplifiers while keeping the same number of unit cells, we expect the GDM-based approach to straightforwardly extend to even

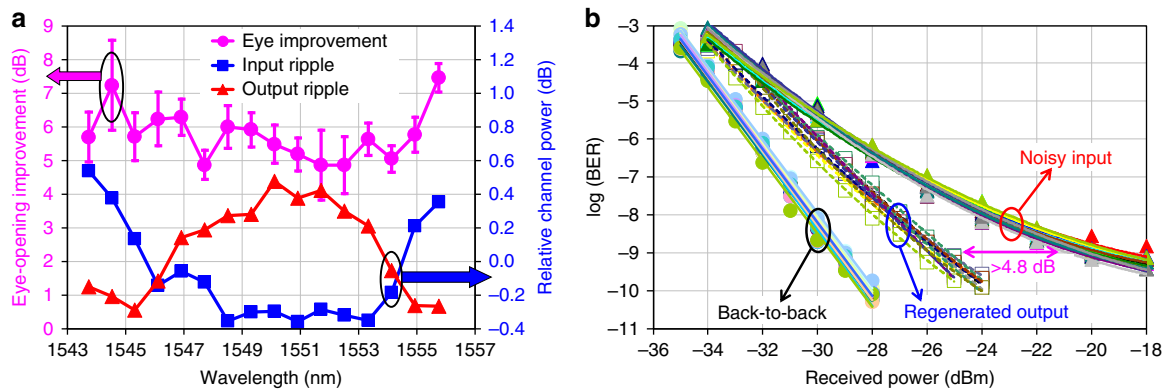


Fig. 7 BER measurements and spectral ripple before and after the stand-alone 2R regenerator. **a** Eye-opening improvements at $\text{BER} = 10^{-9}$ level (purple circles pertaining to the left axis) and spectral ripple (blue squares and red triangles pertaining to the right axis) among the 16 simultaneously regenerated channels. By pre-emphasising the channel powers so that the ripple of the WDM spectrum at the GDM medium input (blue squares) is the inverse of that at the GDM medium output (red triangles), we minimise the differences in optical signal-to-noise ratios and nonlinear phase shifts among the 16 channels due to Raman gain ripple⁶⁶. Error bars are obtained from the parabolic fits to BER curves. **b** BER curves for all 16 channels

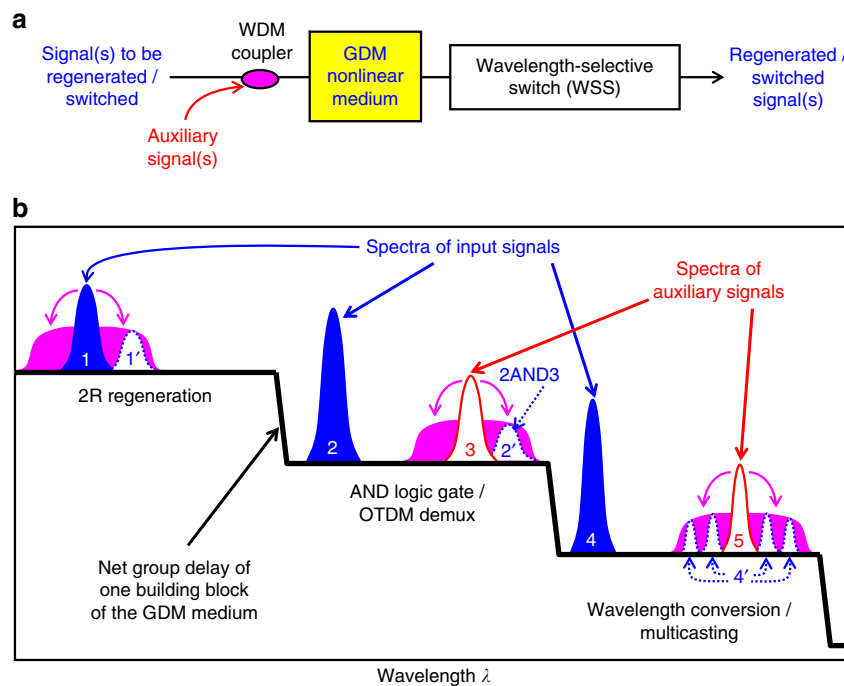


Fig. 8 Schematics of different GDM-enabled all-optical processing applications. These different applications could be potentially implemented simultaneously and independently for signals at multiple wavelengths. **a** Multi-channel signals, combined with auxiliary beams, enter the GDM medium, after which the appropriate output beams are selected by a WSS. **b** Top step of the 'staircase' in the group-delay spectra (black): Mamyshev 2R regenerator implemented for channel 1. Middle step: XPM-based AND operation (or OTDM demultiplexing) between channel 2 and auxiliary signal 3. Bottom step: wavelength conversion/multicasting of channel 4 by its XPM of auxiliary signal 5. Beams 1', 2' and 4' (dotted blue) are selected by the WSS at the output, and the rest of the signals are discarded. Note that the GDM medium permits independent processing of multiple channels for as long as different signal channels (solid blue), along with their respective auxiliary beams (red), occupy different stairsteps of the group-delay staircase spectra

higher channel counts typical for WDM communication systems. Operation at higher symbol rates is also possible after proper rescaling of the signal powers and GDM parameters²¹ and has been numerically validated at 40 Gbps²¹. Although, as a proof of concept of GDM-based multi-channel regeneration, the presented experiments have only focused on the Mamyshev regenerator of OOK signals, we believe there is a clear path to extending this GDM approach to more advanced modulation formats in the future. In particular, the GDM nonlinear medium has been

predicted to enable a multi-channel phase-preserving amplitude regeneration of phase-encoded signals^{49, 50} in a nonlinear amplifying loop mirror (NALM)^{51, 52}, which is also capable of regeneration of multiple amplitude levels⁵³. The GDM nonlinear medium easily permits bi-directional use, which is essential for NALM operation. Phase-preserving amplitude regenerators could further be paired^{54, 55} with potentially multi-channel (see, e.g. refs. 56–60) phase regenerators based on phase-sensitive parametric amplifiers^{61–64} to provide multi-channel processing of

signals encoded with advanced modulation formats, leading to the capacity and reach increase for communication systems⁶⁵. Such an extension of the GDM-assisted multi-channel regeneration to advanced modulation formats presents many challenges, but appears to be a promising direction for future research efforts. Another area for future investigation is in exploring the applications of the GDM nonlinear medium in other all-optical signal-processing schemes, where it may enable multi-channel operation by effectively decoupling the nonlinear interactions taking place within the channel bandwidth of the PGDD from the inter-channel interactions. We show one example of such a potential multi-channel processing scheme in Fig. 8.

Methods

Recirculating-loop experiment. The recirculating-loop setup uses a single fibre + PGDD unit cell with 1.25 km of DCF and $\approx +20$ ps nm⁻¹ net cell dispersion⁴⁰. Two sets of 400-GHz-spaced WDM channels are interleaved to form 12 200-GHz-spaced channels (1542.54...1560.20 nm) modulated by two independent 9.953-Gbps pattern generators (PGs) with slightly different and uncorrelated clock frequencies. We also add a 2-bit delay between the adjacent channels within each set, decorrelating their bit patterns originating from the same PG by a 0.5-km-long DCF. This ensures that we study a realistic worst-case scenario of co-polarised uncorrelated WDM channels, and average the performance over various initial delays between the pulses of neighbouring channels, as required for proper assessment of the inter-channel penalties in the regenerator^{15, 21}. We degrade the channel selected for BER measurements by $\pm 25\%$ amplitude jitter via adding a crosstalk from another laser tuned to the measured channel's wavelength. The remaining WDM channels are not artificially degraded. Each channel's average power is ~ 60 mW at the DCF input. An attenuator after the DCF prevents nonlinear interactions outside the DCF. The signals are injected into the loop by acousto-optic switch AOS1. AOS1 and AOS2 are driven by trains of rectangular pulses in counter-phase: during the loop-loading cycle, AOS1 is in a low-loss state and AOS2 is in a high-loss state; their states are reversed for the rest of the rectangular-wave period (loop recirculation). The net loss and gain in the loop are carefully balanced. Pulsed gate coinciding with timing of a particular circulation in the loop controls the inputs to the optical spectrum analyser (OSA), BER tester and DCA. After five circulations, the regenerated signals are selected, one at a time, by a 0.2-nm-wide tunable OBPF with ~ 0.15 -nm offset from the original signal's wavelength and are subsequently detected by an optically pre-amplified receiver. It is worth noting that recirculating loops are most frequently used to characterise cascaded optical networking and ultra-long-haul transmission, which typically requires 50 or more km of fibre (i.e. round-trip time at least in hundreds of μ s) for reliable operation. In contrast, in our experiment, by using fast (< 50 ns response time) loop switches and diagnostic equipment gates (acousto-optic switches AOS3 and AOS4 in front of the OSA and DCA, respectively, in Fig. 2), as well as an agile clock recovery at the receiver, we have adapted the recirculating loop to work with short round-trip times down to few μ s (several hundred metres of fibre). This experiment used a fibre-Bragg-grating-based PGDD³⁰ (TeraXion ClearSpectrum).

Stand-alone-regenerator experiment. In the stand-alone-regenerator experiment, we use 16 WDM channels (1543.73...1555.75 nm) on a 100-GHz-spaced ITU grid, obtained by combining even and odd 8-channel sets. Since all signals are modulated by the same 10.7-Gbps PRBS, we decorrelate the bit patterns between the even and odd WDM channel sets by 2-km-long single-mode fibre (SMF) in the even-channel path. We also decorrelate the bit patterns within each of the even and odd channel sets by sending the combined signals through 2.5 km of DCF, producing a 5-bit pattern delay between the adjacent channels of each 200-GHz-spaced set. The intra-channel dispersion from this DCF spool is 67%-compensated by a preceding PGDD (set to $+200$ ps nm⁻¹), while the dispersion accumulated between the channels is preserved. To emulate the real noise in transmission, a broadband Nyquist-Johnson thermal noise, generated by several cascaded electronic amplifiers with net frequency range spanning from 50 kHz to 14 GHz, drives separate amplitude modulators (of the same type as those used for data modulation) for even and odd channels and is decorrelated among the channels by the same combination of the 2-km-long SMF and 2.5-km-long DCF. In addition, we decorrelate the clock frequencies of even and odd channels by frequency modulation (FM) of the clock of a single PG, in lieu of employing a second PG. This is done by mixing the original 10.69 GHz sine-wave clock at a radio-frequency (RF) single-sideband modulator with a 30-MHz sine wave, FM-modulated with 50-kHz repetition frequency and ± 100 -kHz frequency deviation, which generates a 10.72-GHz clock with FM, as shown in Fig. 5c. The half-period of FM (10 μ s) roughly corresponds to the delay of the even channels by the 2-km-long SMF and ensures that, after combining, even and odd channels have clocks whose frequency difference constantly changes in the range from -200 to $+200$ kHz, leading to continuous variation of the relative input bit delays between the adjacent 100-GHz-spaced channels from -0.64 to $+0.64$ bit periods over the span of 20- μ s FM period.

After the first EDFA, a 50-to-100-GHz interleaver with 0.25-nm-wide passband suppresses out-of-band amplified spontaneous emission noise. After the second, high-power, EDFA the co-polarised signals enter the Mamyshev regenerator consisting of the GDM medium producing SPM-induced spectral broadening and an OBPF detuned by -0.07 nm from the original channel's centre. In a real system, a spectrally periodic OBPF (comb filter such as an interleaver) can simultaneously handle all WDM channels, whereas we use a single tunable 0.2-nm-wide OBPF, because we only have one receiver. The GDM medium consists of five identical 1-km-long DCF sections and one 1.25-km DCF section near the middle of the GDM medium, all separated by PGDDs. This experiment uses PGDDs based on cascaded Gires-Tournois etalons (Oclaro PowerShaper PS3300), which have flat amplitude response²⁹. The dispersion of each PGDD is set to $+150$ ps nm⁻¹, yielding the residual dispersion for each of four identical (1-km DCF + PGDD) unit cells near $+30$ ps nm⁻¹ optimum⁴⁰ and the residual dispersion of the cell with 1.25-km-long DCF near 0 ps nm⁻¹. Compared to our preliminary experiments²⁶, the residual dispersion of each cell has been increased by 20 ps nm⁻¹ and the pre-compensation (DCF + PGDD preceding the GDM medium) has been changed from 0 to -100 ps nm⁻¹ to produce better regeneration performance. The net intra-channel dispersion of the entire GDM medium including the last piece of 1-km-long DCF is 0 ps nm⁻¹. At the same time, the signals from the adjacent 100-GHz-spaced WDM channels walk off from each other by at least 6 bit periods over the GDM medium length. Each PGDD's loss is ≈ 4 dB, which, together with the loss of the DCF (including DCF-to-SMF splices) and pump/signal WDM couplers, yields the total passive loss of the GDM medium near 35 dB. To compensate it, we use eight Raman pump units (RPUs, each with two wavelengths and two polarisations multiplexed) to bi-directionally pump the GDM medium to transparency (with undepleted pumps). RPU #1 in Fig. 5b has pump wavelengths of 1440 nm and 1455 nm, RPU #2—1443 nm and 1455 nm, RPU #3—#6—1460 nm and 1470 nm, RPU #7—1440 nm and 1462 nm, and RPU #8—1443 nm and 1462 nm. Extra pump/signal 14XX/15XX WDM couplers allow the Raman pump light bypass the lossy PGDDs. The optimum total average signal power entering the GDM medium is 26 dBm (~ 25 mW per channel). At this power the Raman gain is saturated, and the total average signal power at the output of the last 1-km DCF section falls to 23.6 dBm. Compared to our preliminary experiments²⁶, in this setup we have shifted the WDM channel plan toward shorter wavelengths to take advantage of the Raman gain peak of the available pumps, and optimised the Raman pump powers to better equalise the gain. This has increased the minimum (worst-channel) GDM net transmission from -5.6 dB to -3.2 dB and reduced the gain ripple from 2.8 dB to 1.4 dB, yielding considerably less variation of the signal power across the spectrum and along the length of the GDM medium, i.e. better approximating the ideal lossless GDM medium. As a result, we have achieved a 33% increase in the number of WDM channels (from 12 to 16), as well as a better and more uniform regeneration performance among the WDM channels.

Data availability. The data that support the findings of this study are available from the corresponding author upon reasonable request.

Received: 22 August 2016 Accepted: 29 July 2017

Published online: 12 October 2017

References

- Ciarabella, E. Wavelength conversion and all-optical regeneration: achievements and open issues. *J. Lightwave Technol.* **30**, 572–582 (2012).
- Parmigiani, F. et al. Progress in multichannel all-optical regeneration based on fiber technology. *IEEE J. Sel. Top. Quantum Electron.* **18**, 689–700 (2012).
- Leclerc, O., Brindel, P., Bigo, S., Brun-Maunand, E. & Desurvire, E. 2×20 Gbit/s, 3500 km regenerated WDM soliton transmission with all-optical Kerr fibre modulation. *Electron. Lett.* **34**, 199–201 (1998).
- Leclerc, O. et al. Simultaneously regenerated 4×40 Gbit/s dense WDM transmission over 10000 km using single 40 GHz InP Mach-Zehnder modulator. *Electron. Lett.* **36**, 1574–1575 (2000).
- Tan, H. N., Matsuura, M., Katafuchi, T. & Kishi, N. Multiple-channel optical signal processing with wavelength-waveform conversions, pulsewidth tunability, and signal regeneration. *Opt. Express* **17**, 22960–22973 (2009).
- Yu, Y. et al. in *Proc. Optical Fiber Communication Conference*, Paper JWA48 (San Diego, CA, 2010).
- Gavioli, G. & Bayvel, P. in *Proc. 16th Annual Meeting of the IEEE Lasers and Electro-Optics Society*, 2, 896–897 (IEEE, New York, NY, 2003).
- Le, Q. T. et al. WDM compatible 2R regeneration device based on eight-channel saturable absorber module. *Electron. Lett.* **43**, 1305–1306 (2007).
- Bramerie, L. et al. All-optical 2R regeneration with a vertical microcavity-based saturable absorber. *IEEE J. Sel. Top. Quantum Electron.* **18**, 870–883 (2012).
- Cvecek, K. et al. Phase-preserving amplitude regeneration for a WDM RZ-DPSK signal using a nonlinear amplifying loop mirror. *Opt. Express* **16**, 1923–1928 (2008).

11. Ohara, T., Takara, H., Hirano, A., Mori, K. & Kawanishi, S. 40-Gb/s \times 4-channel all-optical multichannel limiter utilizing spectrally filtered optical solitons. *IEEE Photonics Technol. Lett.* **15**, 763–765 (2003).
12. Provost, L., Parmigiani, F., Petropoulos, P. & Richardson, D. J. Investigation of simultaneous 2R regeneration of two 40-Gb/s channels in a single optical fiber. *IEEE Photonics Technol. Lett.* **20**, 270–272 (2008).
13. Vorreau, P. et al. Optical grooming switch with regenerative functionality for transparent interconnection of networks. *Opt. Express* **17**, 15173–15185 (2009).
14. Provost, L. et al. Investigation of four-wavelength regenerator using polarization- and direction-multiplexing. *IEEE Photonics Technol. Lett.* **20**, 1676–1678 (2008).
15. Kouloumentas, C. et al. Four-channel all-fibre dispersion-managed 2R regenerator. *IEEE Photonics Technol. Lett.* **20**, 1169–1171 (2008).
16. Zhou, X. et al. in *Proc. Asia Communications and Photonics Conference*, Paper ASu2A.121 (Hong Kong, 2015).
17. Shah, N. S. M. & Matsumoto, M. 2R regeneration of time-interleaved multiwavelength signals based on higher order four-wave mixing in a fiber. *IEEE Photonics Technol. Lett.* **22**, 27–29 (2010).
18. Wang, J. et al. 4 \times 160-Gbit/s multi-channel regeneration in a single fiber. *Opt. Express* **22**, 11456–11464 (2014).
19. Guan, P. et al. in *Proc. European Conference on Optical Communication*, Paper We.3.6.4 (Valencia, Spain, 2015).
20. Chi, N., Xu, L., Berg, K. S., Tokle, T. & Jeppesen, P. All-optical wavelength conversion and multichannel 2R regeneration based on highly nonlinear dispersion-imbalanced loop mirror. *IEEE Photonics Technol. Lett.* **14**, 1581–1583 (2002).
21. Vasilyev, M. & Lakoba, T. I. All-optical multichannel 2R regeneration in a fiber-based device. *Opt. Lett.* **30**, 1458–1460 (2005).
22. Mamyshev, P. V. in *Proc. European Conference on Optical Communications* 475–476 (Madrid, Spain, 1998).
23. Patki, P. G., Vasilyev, M. & Lakoba, T. I. in *Proc. IEEE LEOS European Winter Topical on Nonlinear Processing in Optical Fibres*, Paper WC2.3 (Innsbruck, Austria, 2009).
24. Patki, P. G., Vasilyev, M. & Lakoba, T. I. in *Proc. IEEE Photonics Society Summer Topical Meeting on Nonlinear Fiber Optics*, Paper WC2.2 (Playa del Carmen, Mexico, 2010).
25. Li, L., Vasilyev, M. & Lakoba, T. I. in *Proc. CLEO Conference*, Paper SM2M.2 (San Jose, CA, 2015).
26. Li, L., Kwon, Y.-B., Campbell, B., Lakoba, T. I. & Vasilyev, M. in *Proc. Optical Fiber Communication Conference*, Paper W4D.4 (Anaheim, CA, 2016).
27. Guan, P. et al. in *Proc. European Conference on Optical Communications*, Post-deadline Paper Th.3.B.3 (Düsseldorf, Germany, 2016).
28. Lunardi, L. M. et al. Tunable dispersion compensation at 40 Gb/s using a multicavity etalon all-pass filter, with NRZ, RZ and CSRZ modulation. *J. Lightwave Technol.* **20**, 2136–2144 (2002).
29. Yang, D., Lin, C., Chen, W. & Barbarossa, G. Fiber dispersion and dispersion slope compensation in a 40-channel 10-Gb/s 3200-km transmission experiment using cascaded single-cavity Gires-Tournois etalons. *IEEE Photonics Technol. Lett.* **16**, 299–301 (2004).
30. Lachance, R. L., Lelievre, S. & Painchaud, Y. in *Proc. Optical Fiber Communications Conference*, Technical Digest Vol. 1, 164–165 (OSA, Washington, D.C., 2003).
31. Eggleton, B. J., Luther-Davies, B. & Richardson, K. Chalcogenide photonics. *Nat. Photonics* **5**, 141–148 (2011).
32. Moss, D. J., Morandotti, R., Gaeta, A. L. & Lipson, M. New CMOS-compatible platforms based on silicon nitride and Hydex for nonlinear optics. *Nat. Photonics* **7**, 597–607 (2013).
33. Madsen, C. K. et al. Integrated all-pass filters for tunable dispersion and dispersion slope compensation. *IEEE Photonics Technol. Lett.* **11**, 1623–1625 (1999).
34. Doerr, C. R., Stulz, L. W., Chandrasekhar, S., Buhl, L. & Pafchek, R. in *Proc. Optical Fiber Communications Conference*, Paper PD FA6 (Anaheim, CA, 2002).
35. Stelmakh, N. & Vasilyev, M. in *Proc. IEEE Photonics Society Summer Topical Meeting on Novel Waveguiding, Structures, and Phenomena*, Paper WB2.5 (Playa del Carmen, Mexico, 2010).
36. Belotti, G. & Bigo, S. Cross-phase modulation suppressor for multispan dispersion-managed WDM transmissions. *IEEE Photonics Technol. Lett.* **12**, 726–728 (2000).
37. Bellotti, G., Bigo, S., Cortès, P.-Y., Gauchard, S. & LaRochelle, S. 10 \times 10 Gb/s Cross-phase modulation suppressor for multispan transmissions using WDM narrow-band fiber Bragg gratings. *IEEE Photonics Technol. Lett.* **12**, 1403–1405 (2000).
38. Wei, X., Liu, X., Xie, C. & Mollenauer, L. F. Reduction of collision-induced timing jitter in dense wavelength-division multiplexing by the use of periodic-group-delay dispersion compensators. *Opt. Lett.* **28**, 983–985 (2003).
39. Mollenauer, L. F. et al. Experimental test of dense wavelength-division multiplexing using novel, periodic-group-delay-complemented dispersion compensation and dispersion-managed solitons. *Opt. Lett.* **28**, 2043–2045 (2003).
40. Lakoba, T. I. & Vasilyev, M. A new robust regime for a dispersion-managed multichannel 2R regenerator. *Opt. Express* **15**, 10061–10074 (2007).
41. Patki, P. G., Stelmakh, V., Annamalai, M., Lakoba, T. I. & Vasilyev, M. in *Proc. Frontiers in Optics/Laser Science XXIII Meeting*, Paper FTHS3 (San Jose, CA, 2007).
42. Kouloumentas, C. et al. All-fiberized dispersion-managed multichannel regeneration at 43 Gb/s. *IEEE Photonics Technol. Lett.* **20**, 1854–1856 (2008).
43. Temprana, E. et al. Overcoming Kerr-induced capacity limit in optical fiber transmission. *Science* **348**, 1445–1448 (2015).
44. Solis-Trapala, K., Pelusi, M. D., Tan, H. N., Inoue, T. & Namiki, S. in *Proc. Optical Fiber Communications Conference*, Paper Th3C.2 (Los Angeles, CA, 2015).
45. Phillips, I. D. et al. in *Proc. Optical Fiber Communications Conference*, Paper M3C.1 (San Francisco, CA, 2014).
46. Sackey, I. et al. Kerr nonlinearity mitigation in 5 \times 28-GBd PDM 16-QAM signal transmission over a dispersion uncompensated link with backward-pumped distributed Raman amplification. *Opt. Express* **22**, 27381–27391 (2014).
47. Narimanov, E. E. & Mitra, P. The channel capacity of a fiber optics communication system: Perturbation theory. *J. Lightwave Technol.* **20**, 530–537 (2002).
48. Ellis, A. D., McCarthy, M. E., Al-Khateeb, M. A. Z. & Sygletos, S. Capacity limits of systems employing multiple optical phase conjugators. *Opt. Express* **23**, 20381–20393 (2015).
49. Lakoba, T. I., Williams, J. R. & Vasilyev, M. NALM-based, phase-preserving 2R regenerator of high-duty-cycle pulses. *Opt. Express* **19**, 23017–23028 (2011).
50. Lakoba, T. I. & Vasilyev, M. On multi-channel operation of phase-preserving 2R amplitude regenerator. *Opt. Commun.* **322**, 114–117 (2014).
51. Boscolo, S., Bhamber, R. & Turitsyn, S. K. Design of Raman-based nonlinear loop mirror for all-optical 2R regeneration of differential phase-shift-keying transmission. *IEEE J. Quantum Electron.* **42**, 619–624 (2006).
52. Cvecek, K., Sponsel, K., Onishchukov, G., Schmauss, B. & Leuchs, G. 2R-regeneration of an RZ-DPSK signal using a nonlinear amplifying loop mirror. *IEEE Photonics Technol. Lett.* **19**, 146–148 (2007).
53. Röthlingshöfer, T. et al. All-optical phase-preserving multilevel amplitude regeneration. *Opt. Express* **22**, 27077–27085 (2014).
54. Li, L. & Vasilyev, M. All-optical 2R regenerator of 16-QAM signals. *Proc. SPIE* **9009**, 900908 (2014).
55. Sorokina, M., Sygletos, S., Ellis, A. & Turitsyn, S. Regenerative Fourier transformation for dual-quadrature regeneration of multilevel rectangular QAM. *Opt. Lett.* **40**, 3117–3120 (2015).
56. Vasilyev, M. Distributed phase-sensitive amplification. *Opt. Express* **13**, 7563–7571 (2005).
57. Tang, R., Devgan, P. S., Grigoryan, V. S., Kumar, P. & Vasilyev, M. In-line phase-sensitive amplification of multi-channel CW signals based on frequency non-degenerate four-wave-mixing in fiber. *Opt. Express* **16**, 9046–9053 (2008).
58. Sygletos, S. et al. A practical phase sensitive amplification scheme for two channel phase regeneration. *Opt. Express* **19**, B938–B945 (2011).
59. Kurosu, T., Gao, M., Solis-Trapala, K. & Namiki, S. Phase regeneration of phase encoded signals by hybrid optical phase squeezer. *Opt. Express* **22**, 12177–12188 (2014).
60. Parmigiani, F., Bottrill, K. R. H., Slavik, R., Richardson, D. J. & Petropoulos, P. in *Proc. European Conference on Optical Communications*, Paper P.3.13 (Valencia, Spain, 2015).
61. Slavik, R. et al. All-optical phase and amplitude regenerator for next-generation telecommunications systems. *Nat. Photonics* **4**, 690–695 (2010).
62. Tong, Z. et al. Towards ultrasensitive optical links enabled by low-noise phase-sensitive amplifiers. *Nat. Photonics* **5**, 430–436 (2011).
63. Kakande, J. et al. Multilevel quantization of optical phase in a novel coherent parametric mixer architecture. *Nat. Photonics* **5**, 748–752 (2011).
64. Mohajerin-Ariaei, A. et al. Phase noise mitigation of QPSK signal utilizing phase-locked multiplexing of signal harmonics and amplitude saturation. *Opt. Lett.* **40**, 3328–3331 (2015).
65. Sorokina, M. A. & Turitsyn, S. K. Regeneration limit of classical Shannon capacity. *Nat. Commun.* **5**, 3861 (2014).
66. Vasilyev, M., Mehendale, M. & Tsuda, S. Optimum pre-emphasis in ultra-long-haul networks. *J. Opt. Netw.* **5**, 159–174 (2006).

Acknowledgements

This work was supported in part by the National Science Foundation grants DMS-0507429/0507540 and ECCS-0925706/0925860. The authors are grateful to V.L. DaSilva,

S. Bickham, and Corning, Inc. for providing the DCF, and to P. Young for lending the second BER analyser.

Author contributions

L.L. and P.G.P. contributed equally to this work. P.G.P. built and characterised the recirculating-loop-based regenerator. L.L. built and characterised the stand-alone regenerator. M.V. supervised the experiments and provided overall technical leadership. T.I.L. did theoretical and numerical modelling/optimisation of the setup. V.S. contributed to design and implementation of the recirculating loop with short time of flight. Y.B.K. and B.D.C. contributed to the design and implementation of Raman-assisted GDM medium. M.A. contributed to writing control and data acquisition software.

Additional information

Competing interests: The authors declare no competing financial interests.

Reprints and permission information is available online at <http://npg.nature.com/reprintsandpermissions/>

Publisher's note: Springer Nature remains neutral with regard to jurisdictional claims in published maps and institutional affiliations.



Open Access This article is licensed under a Creative Commons Attribution 4.0 International License, which permits use, sharing, adaptation, distribution and reproduction in any medium or format, as long as you give appropriate credit to the original author(s) and the source, provide a link to the Creative Commons license, and indicate if changes were made. The images or other third party material in this article are included in the article's Creative Commons license, unless indicated otherwise in a credit line to the material. If material is not included in the article's Creative Commons license and your intended use is not permitted by statutory regulation or exceeds the permitted use, you will need to obtain permission directly from the copyright holder. To view a copy of this license, visit <http://creativecommons.org/licenses/by/4.0/>.

© The Author(s) 2017